Problem Chosen	2023 ShuWei Cup Summary Sheet	Team Control Number
B		2023110120593

Study on the Mechanism of Chemical Pyrolysis Reactions Based on Nonlinear Regression Model and Grey Prediction Model

Summary

In this paper, to explore the differential characteristics and underlying reasons, this paper first analyzes the existing data using trend analysis, correlation analysis, and linear programming. Then, differential analysis is conducted using t-tests and analysis of variance. Finally, a nonlinear regression model is established and validated using residual analysis, demonstrating the rationality and accuracy of the mathematical model.

Question one: Using statistical analysis, Spearman correlation analysis, and trend analysis of linear and quadratic fitting curves for the data. Firstly, we conducted basic observations and statistical analysis of the data in Appendix I. Secondly, by calculating the Spearman correlation coefficients between the four pyrolysis products at different process steps, we constructed a thermodynamic coefficient graph among the indicators. Finally, we used MATLAB to perform linear and polynomial regression fitting on the four pyrolysis products under the pyrolysis processes of three different catalysts。

Question two: Using statistical analysis, Pearson correlation analysis, and trend analysis of data fitting curves. Following the approach in the first problem, we initially conducte statistical analysis of the data in AppendixII. Subsequently, by calculating the Pearson correlation coefficients between the four pyrolysis products at different process steps, we constructed a thermodynamic coefficient graph among the indicators. Finally, we used MATLAB to perform linear and polynomial regression fitting on the pyrolysis products of various gases under the pyrolysis processes of three different catalysts. The results indicate, through the R-value and trends in the graphs, that different catalysts have a significant impact on the formation of pyrolysis gas combinations at different mixing ratios.

Question three: We utilized normal distribution analysis and conducted differential analysis using t-tests and variance analysis. Firstly, we confirmed the normal distribution of the physical indicators through data morphology, thereby meeting the conditions for paired sample t-tests. Subsequently, we performed paired sample t-tests on the physical indicators, revealing significant differences in the yield of high-temperature decomposition gas components between CE and LG under the same proportion of desulfurized ash catalysis. The underlying reasons may be related to chemical reaction mechanisms and kinetic models, which will be elaborated in detail in the fourth section.

Question four: We consulted relevant literature and provided reaction mechanism models and kinetic models. Initially, through the review of pertinent literature, we obtained the reaction mechanism and kinetic models for the desulfurized ash catalyzed reactions of model compounds for CE and LG. These findings have contributed to the explanation of the results in the aforementioned three questions.

Question five: We established a non-linear regression fitting model for prediction, alongside accuracy testing and sensitivity analysis. Initially, we conducted non-linear regression fitting, such as exponential, logarithmic, and multiple regression fitting, based on the data trends in the literature and the Appendix analyzed in the first three questions, to predict the yield and quantity of pyrolysis products. Subsequently, we performed accuracy testing and sensitivity analysis on the established prediction models, revealing their high accuracy. Finally, we use Grey Prediction Model to predict the trend.

Keywords: **Spearman and Pearson correlation analysis, linear and quadratic fitting, t-tests and variance analysis, non-linear regression fitting model,Grey Prediction Model**

Content

1. Introduction

1.1 Background

The escalating global demand for renewable energy has propelled biomass energy into the spotlight. Cotton stalks, an abundant agricultural waste, stand out as a vital biomass resource due to their rich cellulose and lignin content. However, optimizing the quality and yield of pyrolysis products from cotton stalks demands a nuanced understanding of factors like pyrolysis temperature and catalyst influence. This study delves into the mechanisms and properties of cotton stalk pyrolysis products, emphasizing the catalytic impact during the pyrolysis process. This exploration is pivotal for the efficient utilization and sustainable development of cotton stalks.

2. Problem analysis

2.1 Analysis of question one

Problem 1 requires an analysis of the relationship between the yield of pyrolysis products (tar, water, coke residue, and syngas) and the mixing ratio of desulfurized ash/cotton stalks (DFA/CS), desulfurized ash/cellulose (DFA/CE), and desulfurized ash/lignin (DFA/LG) under different blending ratios.We first conducted a trend analysis of the data in Appendix 1, initially establishing line graphs to observe and compare the trends of the production of the four pyrolysis products under different blending ratios. Subsequently, we quantitatively analyzed the strength of the relationship between the blending ratio and the yield of each pyrolysis product through correlation analysis. Finally, using MATLAB, we plotted scatter diagrams illustrating the relationship .

2.2 Analysis of question two

Problem 2 requires an analysis of the impact of different blending ratios on the yield of each pyrolysis gas within three pyrolysis combinations, as well as an explanation of the influence on each group of pyrolysis gases, based on the data in Appendix 2. Similar to the first question, we conducted a trend analysis of the data in and we quantitatively analyzed the strength of the relationship between the blending ratio and the yield of each pyrolysis gas through correlation analysis. Finally, using MATLAB, we plotted scatter diagrams illustrating the relationship.

2.3 Analysis of question three

Problem 3 requires us to determine whether there is a significant difference in the yield of pyrolysis products and the composition of pyrolysis gases between CE and LG under the catalytic action of desulfurized ash at the same proportion, and to provide reasons for our findings. We conducted a normality test on the samples and found that the data indeed followed a normal distribution. Subsequently, we performed a paired t-test to analyze the differences in the data, revealing a highly significant difference in the yield between CE and LG. Furthermore, we utilized one-way analysis of variance (ANOVA) to conduct differential analysis, and the conclusion was consistent, further reinforcing the accuracy of the result.

2.4 Analysis of question four

Problem four requires the establishment of a catalytic reaction mechanism model and a kinetic model for desulfurization ash on model compounds like CE and LG. We

employ a literature review approach, comparing our data and analysis with relevant references. Through this analysis, we derive accurate kinetic and catalytic mechanism models, finding mathematical formulas consistent with the yields of the four pyrolysis products and individual gas production in the preceding three questions.

2.5 Analysis of question five

Problem five tasks us with predicting the yield of pyrolysis products using mathematical modeling or AI learning within defined constraints. This necessitates the establishment and validation of a predictive model. Leveraging insights from literature and integrating data analysis from questions four and three, we will construct a nonlinear regression model and Grey Prediction Model. Subsequently, we will assess the model's accuracy and provide an explanation for the predicted accuracy.

3. Symbol and Assumptions

3.1 Symbol Description

Category	Meaning
m_0	Quality of the sample material
m_t	Mass of the sample at time t
m_∞	Final remaining quantit
$f(\alpha)$	refer to reaction mechanism function
$g(\alpha)$	refer to reaction mechanism function
A	Pre-exponential factor
$\mathrm{cov}(X, Y)$	covariance
δ_X	Standard deviation

3.2 Fundamental assumptions

In order to simplify the given problem and modify it to a more suitable simulation. In reality, we make the following basic assumptions. Every assumption has a valid reason.

(1) Homogeneous Reaction Environment Assumption: Assume that the reaction takes place homogeneously throughout the entire reaction system, neglecting potential local variations.
(2) Ideal Mixing Assumption: Assume that substances in the reaction system are ideally mixed, disregarding potential non-uniformities or local concentration differences.
(3) Steady-State Reaction Process Assumption: Assume that the reaction system is in a steady state throughout the entire process, meaning that parameters such as reaction rates do not exhibit significant changes over time.

4. Model

4.1 Modeling of question one

4.1.1Statistical analysis

Based on the data provided in Appendix A, a trend analysis was conducted on three charts, examining the general trends in the yields of four products under different mixing ratios. Firstly, trend results obtained through line charts plotted in Excel are illustrated in

the following figure:

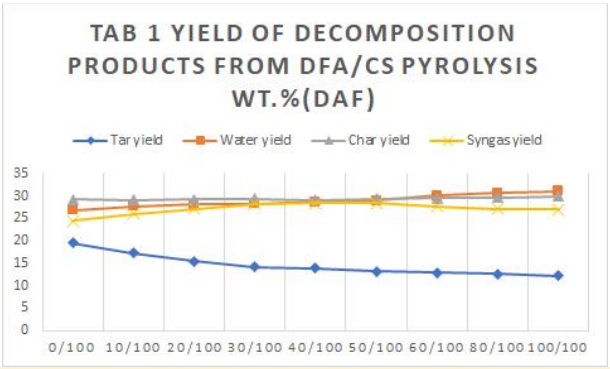

Tab 1 Yield of Decomposition Products from DA/CS Pyrolysis wt.%(daf)

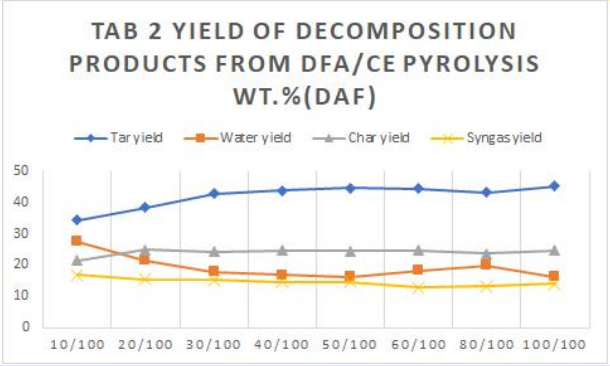

Tab 2 Yield of Decomposition Products from DFA/CE Pyrolysis wt.%(daf)

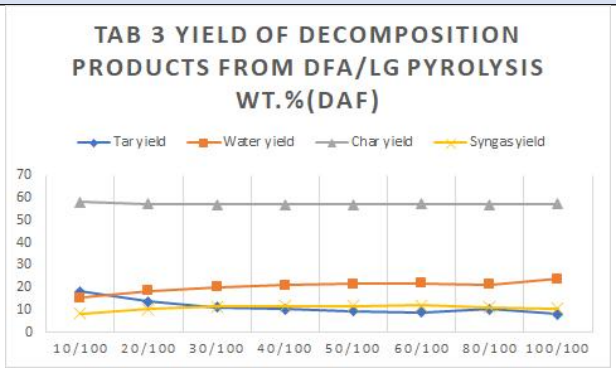

Tab 3 Yield of Decomposition Products from DFA/LG Pyrolysis wt.%(daf)

Chart Explanation:

Upon a comprehensive analysis of the above charts, it is evident that there exists a certain correlation and variation between the yields of pyrolysis products under different pyrolysis combinations and the corresponding mixing ratios.

Specific Result Analysis:

1.In the trend of DFA/CS in TAB1, it can be roughly analyzed that the petroleum yield is negatively correlated with the mixing ratio of this pyrolysis combination, indicating that as the input of DFA increases, the petroleum yield decreases. The water yield shows a positive correlation with the mixing ratio of this pyrolysis combination, meaning that with an increased input of DFA, the water yield decreases.

2.In the trend of DFA/FA in TAB2, it can be roughly analyzed that the petroleum yield is positively correlated with the mixing ratio of this pyrolysis combination, meaning that as the mixing ratio increases, the petroleum yield increases. The water yield is negatively correlated with the mixing ratio of this pyrolysis combination, indicating that with an increased mixing ratio, the water yield decreases.

3.In the trend of DFA/LG in TAB3, it can be roughly analyzed that the petroleum yield is negatively correlated with the mixing ratio of this pyrolysis combination, indicating that as the mixing ratio increases, the petroleum yield

decreases. The water yield shows a slight positive correlation with the mixing ratio of this pyrolysis combination, indicating that with an increased mixing ratio, the water yield slightly increases.

4.1.2 Spearman correlation analysis

Quantitative analysis of the relationship strength between the mixing ratio and the yields of various pyrolysis products is performed using the Spearman rank correlation coefficient.

Model Establishment:

Principle of Spearman Correlation Analysis: Spearman correlation analysis does not require a specific distribution of the original variables and belongs to non-parametric statistical methods [1]. Basic principles:

Spearman rank correlation uses the rank correlation coefficient (r_s) to illustrate the degree and direction of the linear correlation between variables. The basic idea is to rank the n pairs of observed values (X_i, Y_i) (where (i = 1, 2, …, n)) in ascending order separately, with (P_i) representing the rank of (X_i), (Q_i) representing the rank of (Y_i), and ($d_i = P_i - Q_i$) representing the consistency of the rank order of variables X and Y, reflecting the size of the difference between (P_i) and (Q_i). In general, (r_s) values range from -1 to 1. A positive (r_s) value indicates a positive correlation, a negative (r_s) value indicates a negative correlation, and an absolute (r_s) value of zero indicates no correlation. The absolute value of (r_s) between 0.8 and 1.0 indicates a very strong correlation, between 0.6 and 0.8 indicates a strong correlation, between 0.4 and 0.6 indicates a moderate correlation, between 0.2 and 0.4 indicates a weak correlation, and between 0.0 and 0.2 indicates a very weak or no correlation.

Correlation coefficient heatmaps are presented below:

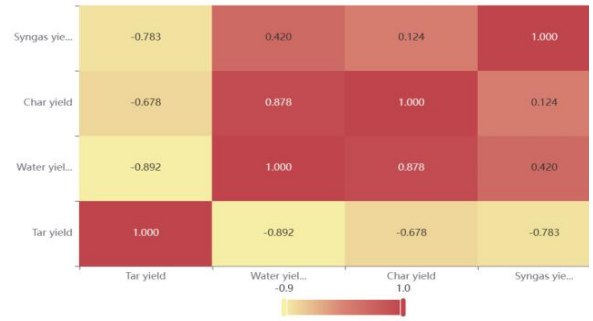

Table 4-1
Thermodynamic diagram in DFA/CS

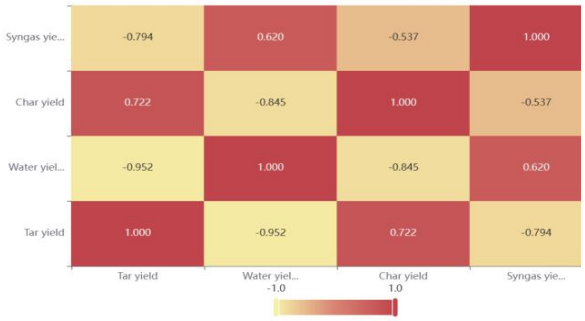

Table 4-2
Thermodynamic diagram in DFA/CE

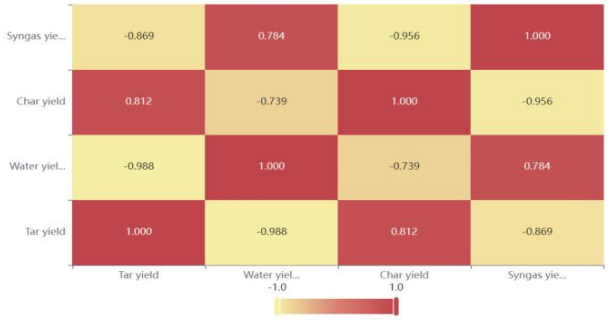

Table 4-3:Thermodynamic diagram in DFA/LG

Graphical explanation:

The figure illustrates the correlation coefficient values in the form of a heatmap, primarily using color depth to indicate the magnitude of the values.

Results analysis:

1.In Table 4-1, for the pyrolysis reaction of DFA/CS, there is a significant positive correlation between water yield and petroleum yield, indicating a highly pronounced influence between the two.

2.In Table 4-2, for the pyrolysis reaction of DFA/CE, a substantial positive correlation is observed between water yield and petroleum yield, signifying a significant impact.

3.In Table 4-3, for the pyrolysis reaction of DFA/LG, a notable negative correlation exists between water yield and petroleum yield, indicating a relatively significant influence.

4.There is a strong negative correlation between petroleum yield and water yield, while there is a significant positive correlation between tar and char. Some noteworthy influences are observed among the four pyrolysis products.

4.1.3 Data Fitting Analysis:

Specifically, we will use the four yields (tar, water, char residue, syngas) as dependent variables and the mixing ratio as the independent variable. Through MATLAB, we will create scatter plots and establish linear and polynomial fitting models. The expressions for the fitted data for the three sets are as follows:

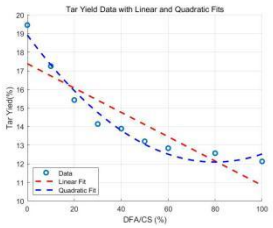

Tar yield in DFA/CS

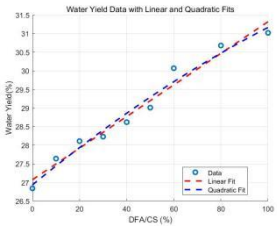

Water yield in DFA/CS

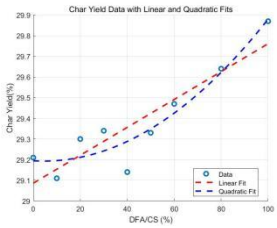

Char yield in DFA/CS

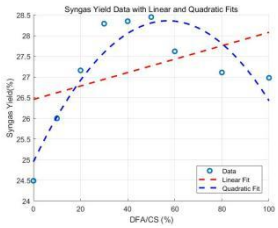

Syngas yield in DFA/CS

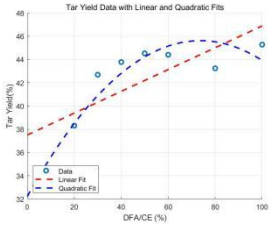

Tar yield in DFA/CE

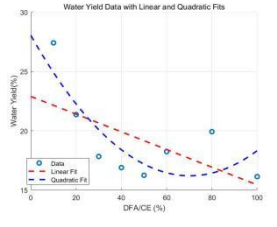

Water yield in DFA/CE

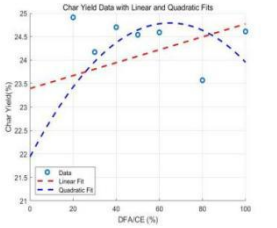

Char yield in DFA/CE

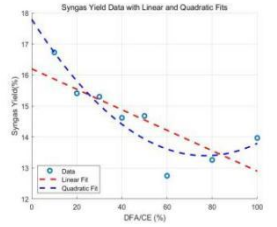

Syngas yield in DFA/CE

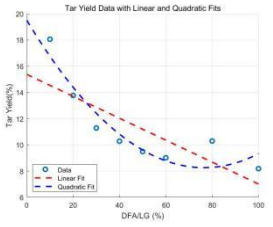

Tar yield in DFA/LG

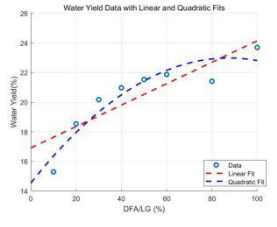

Water yield in DFA/LG

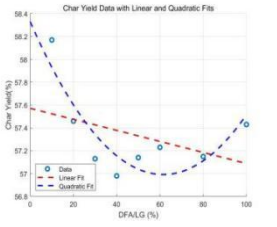

Char yield in DFA/LG

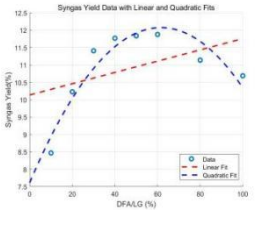

Syngas yield in DFA/LG

Result analysis:

1.The relationship between the yields of the four different products under three different thermal decomposition combinations and varying feed ratios is not linear. Considering the complexity of the chemical reaction process and reaction mechanisms, a detailed analysis of the reasons will be conducted in the fourth question.

2.The trends in the yields of the four different products (tar, water, char residue, syngas) under three different thermal decomposition combinations are distinct, as evident in the line chart analysis.

3.The R-values and trends in the graphs clearly indicate that the presence of a demineralization agent indeed plays a significant role in promoting the pyrolysis of cotton stalks, cellulose, and lignin, and the impact is substantial.

4.2 Modeling of question three

Building on the solutions to the first question, the second question follows the same approach and analytical methods.

4.2.1 Statistical analysis

Based on the data in Appendix Ⅱ, trend analyses were conducted for each of the three charts to observe the overall trends in gas product yields under different mixing ratios. Initially, trend results obtained through Excel line charts are shown in the figure：

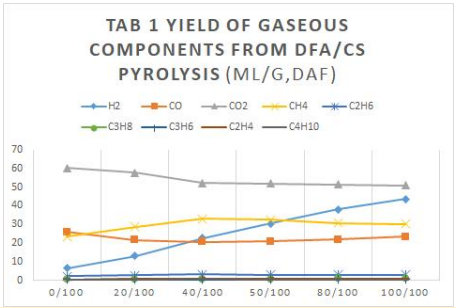

Tab 1 Yield of Gaseous Components from DFA/CS Pyrolysis (mL/g,daf)

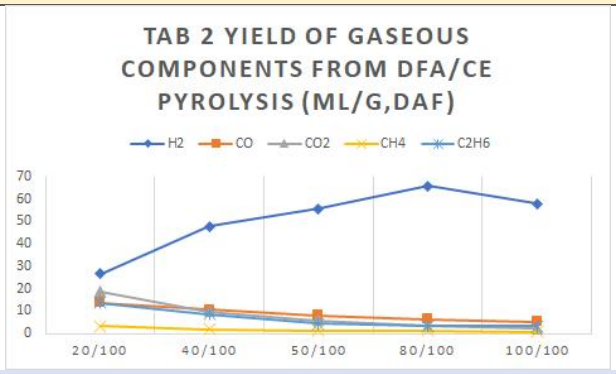

Tab 2 Yield of Gaseous Components from DFA/CE Pyrolysis (mL/g,daf)

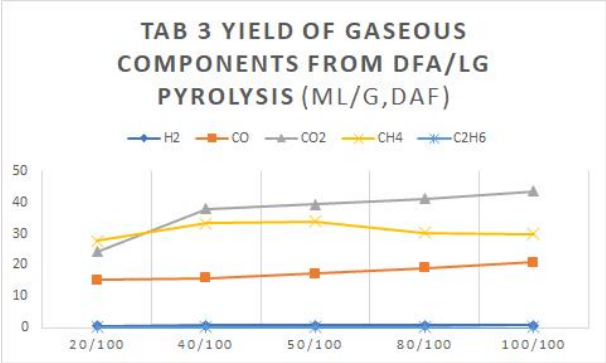

Tab 3 Yield of Gaseous Components from DFA/LG Pyrolysis (mL/g,daf)

Results Analysis:

1.For TAB1DFA/CS's thermal decomposition reaction, it can be observed that CO2 and CO show a decreasing trend with an increase in feed ratio, indicating a negative correlation between the production of these gases and the feed ratio. Meanwhile, the production of H2 gas increases significantly with the increase in the feed ratio, indicating a substantial positive correlation.

2.In the thermal decomposition reaction of TAB2DFA/CE, the production of H2 shows a general positive correlation with the increase in feed ratio, although not following a linear pattern. Conversely, the production of the other three gases decreases notably with the increase in feed ratio, demonstrating a strong negative correlation.

3.In the thermal decomposition reaction of TAB3DFA/LG, it is evident that the production of CO and CO2 decreases with the increase in feed ratio, displaying a strong positive correlation. The production of CH4 gas shows a fluctuating trend with the increase in feed ratio, indicating a significant impact. The production of C2H6 remains relatively stable with the increase in feed ratio, suggesting a weaker correlation.

4.Through a comprehensive comparative analysis of the aforementioned three graphs, it is evident that the feed ratio in each set of thermal decomposition combinations significantly influences the yield, showing a strong correlation. Among the gases produced in each thermal decomposition set, H2 is most affected, while C2H6 is least affected.

4.2.2 Correlation Analysis

The Pearson correlation coefficient is applicable to normally distributed continuous variables.

Based on the preprocessing of data in Appendix Ⅱ, prior to conducting Pearson correlation analysis, it is essential to perform normality tests for each indicator, specifically for the gas production in the three thermal decomposition reactions. The results obtained from the normality distribution tests are as follows:

The Pearson correlation coefficient between variables is defined as the covariance divided by the product of the standard deviations:

$$\rho_{XY} = \frac{\mathrm{cov}(X,\ Y)}{\delta_X \delta_Y} = \frac{\Sigma_{i=1}^{n}\left(\frac{X_i - E(X)}{\delta_X}\right) - \left(\frac{Y_i - E(Y)}{\delta_Y}\right)}{n} \tag{1}$$

$$\delta_X = \frac{\sqrt{\Sigma_{i=1}^{n}\left(X_i - E(X)\right)^2}}{n}\delta_Y, \delta_Y = \frac{\sqrt{\Sigma_{i=1}^{n}\left(Y_i - E(Y)\right)^2}}{n} \quad (2)$$

From the above graphs, it is evident that the data for gas production in the three different thermal decomposition reactions exhibit a "bell-shaped" distribution, resembling a normal distribution curve. Therefore, it can be considered that the normality assumption for distribution is satisfied. Subsequently, we assess the linearity between indicators by calculating the Pearson correlation coefficients. The heatmaps illustrating the three different thermal decomposition reactions, generated using SPSS, are presented below:

Table 4-4
Thermodynamic diagram in DFA/CS

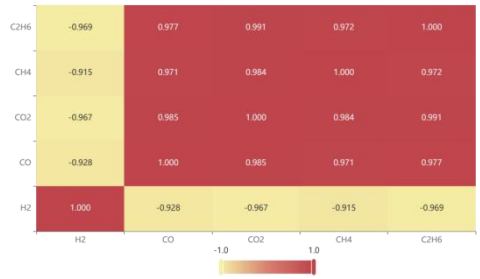

Table 4-5
Thermodynamic diagram in DFA/CE

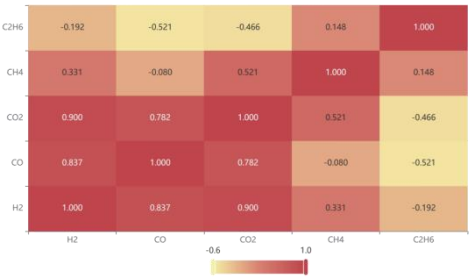

Table 4-6
Thermodynamic diagram in DFA/LG

Graphical explanation:

The figure above depicts the values of correlation coefficients in the form of a heatmap, where the color depth represents the magnitude of the values.

Results Analysis:

1.In Table 4-4, significant correlations are observed among gases in the first set of pyrolysis reactions (DFA/CS). The negative correlation index between CH4 and C2H6 with CO2 and CO is the largest, while the positive correlation between C2H6, CH4, and C3H6, C2H4 is the strongest.

2.In Table 4-5, for the second set of pyrolysis reactions (DFA/CA), all correlation coefficients are greater than 0.9, indicating a strong correlation among gas yields. Hydrogen shows a very strong negative correlation with the yields of all other gases, while there is a very strong positive correlation among the yields of the other gases.

3.In Table 4-6, a strong positive correlation exists between H2 and CO2,

significant at a 1% significance level. There is also a significant positive correlation between H2 and CO, but at a 5% significance level. The correlations between other variables are weaker or statistically insignificant.

4.The three heatmaps illustrate a strong correlation among the yields of most gases in the three pyrolysis reactions, indicating a significant impact on the generation of each gas. Specifically, there is a strong negative correlation between H2 and CO2 at a significance level of 1%. There is a highly significant positive correlation between CH4 and C2H6, and a weaker correlation between CO and CO2.

4.2.3 Data Fitting Analysis

In a similar manner to Problem 1, relationships between the yields of various gases and the input ratio of catalysts under three different pyrolysis combinations were illustrated using MATLAB. The expressions for the fitted data for the three sets are as follows:

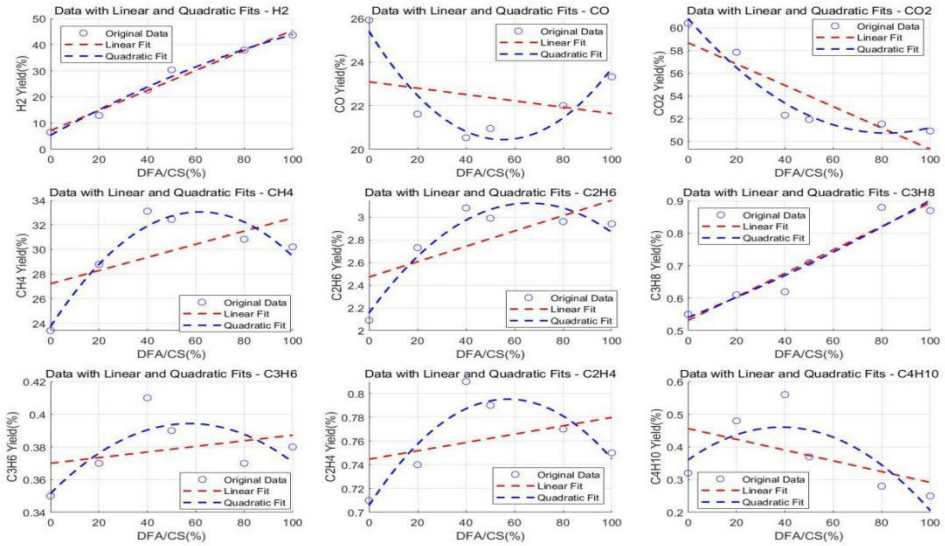

DFA/CSProduction of each gas in pyrolysis reaction

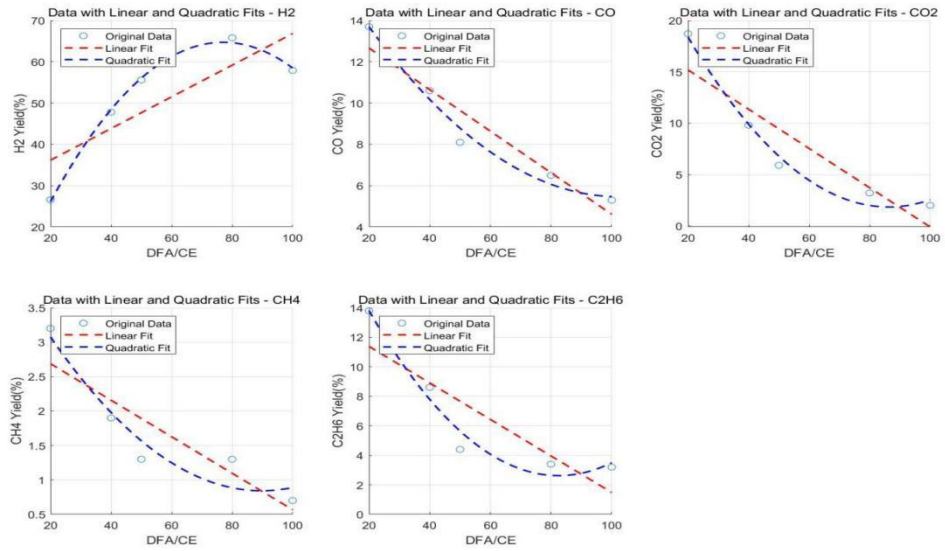

DFA/CEProduction of each gas in pyrolysis reaction

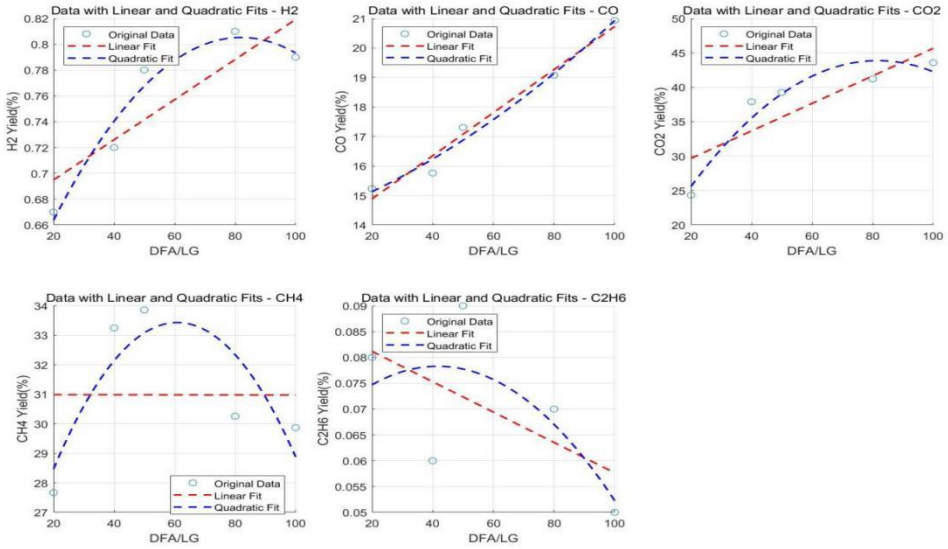

DFA/LGProduction of each gas in pyrolysis reaction

Results Analysis:

1.Under three different pyrolysis combinations, the relationship between the yields of different gases for each pyrolysis combination at different feed ratios shows a low correlation with linear models. Considering the complex chemical reaction processes and factors related to reaction mechanisms among these three types of pyrolysis reactions, a detailed analysis of the reasons will be conducted in the fourth question.

2.The trends in the yields of four different products (tar, water, char, syngas) under three different pyrolysis combinations are distinct, as reflected in the line graph analysis.

3.Through the R-values and trends in the graphs, it is evident that the catalyst removal plays a significant role in promoting the pyrolysis of cotton stalks, cellulose, and lignin, with a considerable impact.

4.3 Modeling of question three

4.3.1 Normality Test

Before conducting differential analysis of the data, a normality distribution test was performed on various indicators. For the four tables in Attachment II, a normality distribution test was conducted for the yields of four pyrolysis products and several pyrolysis gases under different pyrolysis reaction groups. The obtained images are shown below:

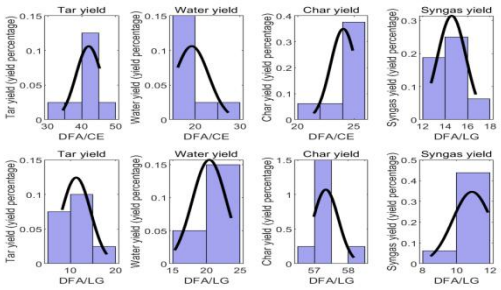

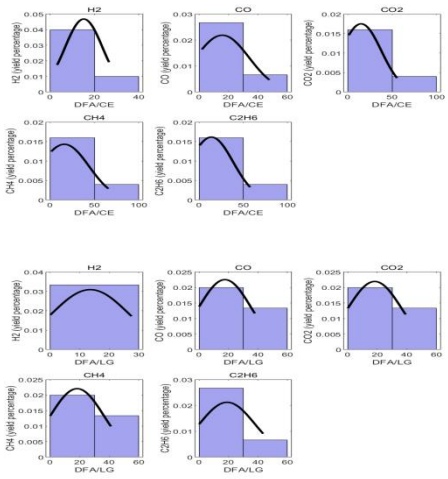

Table 4-7

Table 4-7 indicates that the data for each quantitative indicator in Attachments 1 and 2 exhibit a "bell-shaped" distribution and align with the trend line of normal distribution. Therefore, it is considered that the yields of CE and LG pyrolysis products and pyrolysis gas components follow a normal distribution, enabling independent sample t-tests for differential analysis.

4.3.2 Paired Sample t-test

The t-test compares the means of two sets of quantitative data. The prerequisite for the t-test is that the data come from normally distributed populations and satisfy independence and homogeneity of variance. In the preceding section, verification has already been done for normality. What remains is the condition of homogeneity of variance. Homogeneity of variance is not a strict requirement because t-statistics can be constructed for both homogeneous and non-homogeneous variances, with only a difference in form.

The paired sample t-test is used to compare the means of dependent samples (where the observed values in two sample groups are related). This method is often used in studies where dependent samples come from the same group or system. After the normality test, paired t-tests were conducted to determine if the P-value indicates significance (P < 0.05). If significant, the null hypothesis is rejected, suggesting a difference between paired samples; otherwise, no significant difference is observed between paired samples.

The basic calculation process is as follows:

1.Difference：

$$D_i = X_{1i} - X_{2i} \tag{3}$$

2.Mean Difference：

$$\overline{D} = \frac{\Sigma D_i}{n} \tag{4}$$

3.Standard Deviation of Differences：

$$S_D = \sqrt{\frac{\Sigma(D_i - \overline{D})^2}{(n-1)}} \tag{5}$$

4.Standard Error：

$$S_E = \frac{S_D}{\sqrt{n}} \tag{6}$$

5.t-statistic：

$$t = \frac{D}{S_E} \tag{7}$$

6.Degrees of Freedom：

$$D_f = n - 1 \quad (8)$$

7.P-value：Use the T-distribution table or software (such as Excel, Python, R, etc.) to find the p-value corresponding to the T-value.

Based on SPSS:

Pairing variable	Mean ± standard deviation			t	df	P	Cohen's d
	Pair1	Pair2	Pairing difference (pairing 1- pairing 2)				
CE Tar yield paired with LG Tar yield	42.082±3.764	11.3±3.207	30.782±0.557	12.52	7	0.000***	4.426
CE Water yield paired with LG Water yield	19.262±3.759	20.435±2.539	-1.173±1.22	-0.538	7	0.607	0.19
CE Char yield paired with LG Char yield	24.065±1.141	57.336±0.373	-33.271±0.768	-64.763	7	0.000***	22.897
CE Syngas yield paired with LG Syngas yield	14.59±1.271	10.929±1.153	3.661±0.118	4.621	7	0.002***	1.634

Pairing variable	Mean ± standard deviation			t	df	P	Cohen's d
	Pair1	Pair2	Pairing difference (pairing 1- pairing 2)				
H2 from CE paired with H2 from LG	50.74±14.942	0.754±0.058	49.986±14.884	7.509	4	0.002***	3.358
CO from CE paired with CO from LG	8.84±3.364	17.661±2.365	-8.821±0.999	-3.497	4	0.025**	1.564
CO2 from CE paired with CO2 from LG	7.92±6.73	37.262±7.526	-29.342±-0.796	-4.629	4	0.010***	2.07
CH4 from CE paired with CH4 from LG	1.68±0.95	30.982±2.557	-29.302±-1.607	-21.177	4	0.000***	9.471
CE C2H6 yield paired withC2H6 from LG	6.68±4.54	0.07±0.016	6.61±4.524	3.259	4	0.031**	1.457

Note: ***, ** and * represent significance levels of 1%, 5% and 10% respectively

Chart Explanation:

The table above showcases the results of the model testing, including mean values, standard deviation, t-values, degrees of freedom, and significance levels (P-values).

1. Analyzing the significance P of each pair of matched samples.

2.If significance is evident, rejecting the null hypothesis indicates differences among each pair of matched samples. Conversely, non-significance suggests no significant differences among each pair of matched samples.

3.Cohen's d value: Represents the effect size, with values below 0.2 indicating a very small difference, [0.2, 0.5) indicating a small difference, [0.5, 0.8) indicating a moderate difference, and values above 0.8 indicating a very large difference.

Results Analysis:

In summary, except for water yield, when comparing the thermal gas component yields between CE and LG, there are significantly large differences across all aspects of gas production."

4.3.3 One-Way Analysis of Variance

One-Way Analysis of Variance (ANOVA) is a statistical method used to compare whether the means among multiple groups are equal. It is an inferential statistical technique commonly employed to investigate whether a single factor significantly influences a dependent variable. In the context of mathematical modeling, ANOVA serves to test whether there are significant differences in means among different groups, aiding researchers in understanding the extent to which various factors impact the observed variable.

The fundamental computation process is outlined below:

1.Total Sum of Squares (SST):

$$SST = SSB + SSW \quad (8)$$

2.Calculation Formula for the F-statistic (F):

$$F = MSB / MSW \quad (9)$$

Here, MSB represents the between-group mean square, and MSW represents the within-group mean square.

3.Between-Group Mean Square (MSB):

$$MSB = SSB / (k-1) \quad (10)$$

Here, (k) is the number of groups.

4.Within-Group Mean Square (MSW):

$$[\ MSW = SSW / (N-k)\ ] \quad (11)$$

Here, (N) is the total sample size.

These computations can be performed using SPSS to obtain the results:

Variable Name	Variable Value	Sample Size	Mean	Standard Deviation	Variance Test
CE Tar yield	10/100	1	34.42	0.000	F=0.000 P=0.000
	20/100	1	38.31	0.000	
	30/100	1	42.69	0.000	
	40/100	1	43.78	0.000	
	50/100	1	44.53	0.000	
	60/100	1	44.41	0.000	
	80/100	1	43.24	0.000	
	100/100	1	45.28	0.000	
LG Tar yield	10/100	1	18.06	0.000	F=0.000 P=0.000
	20/100	1	13.77	0.000	
	30/100	1	11.29	0.000	
	40/100	1	10.28	0.000	
	50/100	1	9.49	0.000	
	60/100	1	9.02	0.000	
	80/100	1	10.3	0.000	
	100/100	1	8.19	0.000	
CE Water yield	10/100	1	27.42	0.000	F=0.000 P=0.000
	20/100	1	21.37	0.000	
	30/100	1	17.84	0.000	
	40/100	1	16.9	0.000	
	50/100	1	16.25	0.000	
	60/100	1	18.25	0.000	
	80/100	1	19.93	0.000	
	100/100	1	16.14	0.000	
LG Water yield	10/100	1	15.3	0.000	F=0.000 P=0.000
	20/100	1	18.54	0.000	
	30/100	1	20.17	0.000	
	40/100	1	20.97	0.000	
	50/100	1	21.53	0.000	
	60/100	1	21.87	0.000	
	80/100	1	21.41	0.000	
	100/100	1	23.69	0.000	
CE Char yield	10/100	1	21.43	0.000	F=0.000 P=0.000
	20/100	1	24.91	0.000	
	30/100	1	24.17	0.000	
	40/100	1	24.7	0.000	
	50/100	1	24.54	0.000	
	60/100	1	24.59	0.000	
	80/100	1	23.57	0.000	
	100/100	1	24.61	0.000	
LG Char yield	10/100	1	58.17	0.000	F=0.000 P=0.000
	20/100	1	57.46	0.000	
	30/100	1	57.13	0.000	
	40/100	1	56.98	0.000	
	50/100	1	57.14	0.000	
	60/100	1	57.23	0.000	
	80/100	1	57.15	0.000	
	100/100	1	57.43	0.000	
CE Syngas yield	10/100	1	16.73	0.000	F=0.000 P=0.000
	20/100	1	15.41	0.000	
	30/100	1	15.3	0.000	
	40/100	1	14.62	0.000	
	50/100	1	14.68	0.000	
	60/100	1	12.75	0.000	
	80/100	1	13.26	0.000	
	100/100	1	13.97	0.000	
LG Syngas yield	10/100	1	8.47	0.000	F=0.000 P=0.000
	20/100	1	10.23	0.000	
	30/100	1	11.41	0.000	
	40/100	1	11.77	0.000	

Variable Name	Variable Value	Sample Size	Mean	Standard Deviation	Variance Test
H2 from CE	20/100	1	26.6	0.000	F=0.000 P=0.000
	40/100	1	47.8	0.000	
	50/100	1	55.6	0.000	
	80/100	1	65.8	0.000	
	100/100	1	57.9	0.000	
H2 from LG	20/100	1	0.67	0.000	F=0.000 P=0.000
	40/100	1	0.72	0.000	
	50/100	1	0.78	0.000	
	80/100	1	0.81	0.000	
	100/100	1	0.79	0.000	
CO from CE	20/100	1	13.7	0.000	F=0.000 P=0.000
	40/100	1	10.6	0.000	
	50/100	1	8.1	0.000	
	80/100	1	6.5	0.000	
	100/100	1	5.3	0.000	
CO from LG	20/100	1	15.23	0.000	F=0.000 P=0.000
	40/100	1	15.76	0.000	
	50/100	1	17.305	0.000	
	80/100	1	19.075	0.000	
	100/100	1	20.935	0.000	
CO2 from CE	20/100	1	18.7	0.000	F=0.000 P=0.000
	40/100	1	9.8	0.000	
	50/100	1	5.9	0.000	
	80/100	1	3.2	0.000	
	100/100	1	2	0.000	
CO2 from LG	20/100	1	24.35	0.000	F=0.000 P=0.000
	40/100	1	37.91	0.000	
	50/100	1	39.26	0.000	
	80/100	1	41.23	0.000	
	100/100	1	43.56	0.000	
CH4 from CE	20/100	1	3.2	0.000	F=0.000 P=0.000
	40/100	1	1.9	0.000	
	50/100	1	1.3	0.000	
	80/100	1	1.3	0.000	
	100/100	1	0.7	0.000	
CH4 from LG	20/100	1	27.67	0.000	F=0.000 P=0.000
	40/100	1	33.25	0.000	
	50/100	1	33.86	0.000	
	80/100	1	30.26	0.000	
	100/100	1	29.87	0.000	
CE C2H6 yield	20/100	1	13.8	0.000	F=0.000 P=0.000
	40/100	1	8.6	0.000	
	50/100	1	4.4	0.000	
	80/100	1	3.4	0.000	
	100/100	1	3.2	0.000	
C2H6 from LG	20/100	1	0.08	0.000	F=0.000 P=0.000
	40/100	1	0.06	0.000	
	50/100	1	0.09	0.000	
	80/100	1	0.07	0.000	
	100/100	1	0.05	0.000	

50/100	1	11.84	0.000
60/100	1	11.88	0.000
80/100	1	11.14	0.000
100/100	1	10.69	0.000

Note: ***, ** and * represent significance levels of 1%, 5% and 10% respectively

Results Analysis:

Based on the above findings, obtaining a P-value less than 0.05 leads to the conclusion that there is a significant difference between the levels of the factor. We have grounds to reject the null hypothesis, suggesting that, at this confidence level, the factor significantly influences the observed outcomes. The obtained numerical value is well below 0.05, thus supporting a conclusion similar to that of a paired sample t-test, confirming the presence of a significant difference.

4.4 Modeling of question four

4.4.1 Establishment of Catalytic Reaction Mechanism Models

4.4.1.1: Reaction mechanism of desulfurization ash on the catalytic reaction products of model compounds[2]

To investigate the directed catalytic effect of desulfurization ash on the pyrolysis products of cotton stalks, CE and LG were chosen as model compounds representing cellulose and lignin components in cotton stalks. The ratios of products under different blending ratios of DFA/CE and DFA/LG, as created using MATLAB for DFA/CE and DFA/LG, are illustrated in the graph below.

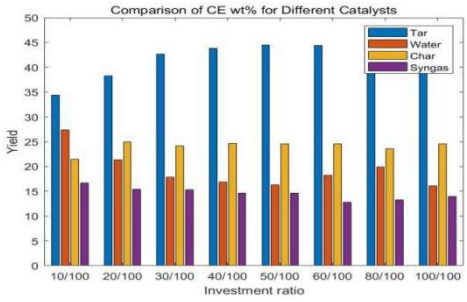

Table 4-8

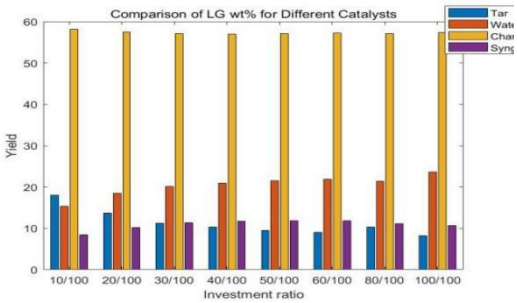

Table 4-9

From Table 4-8, it is observed that tar yields are highest in CE pyrolysis. During the pyrolysis of cellulose, the process produces low molecular weight oligosaccharides and aldehyde-ketone oxidation products, leading to the cracking reaction, generating volatile gases and liquid products, including tar. As DFA/CE increases, tar yield continues to rise, indicating that desulfurization promotes the cracking reaction of oligosaccharides and aldehyde-ketone oxidation products. Cellulose undergoes dehydration reactions during pyrolysis, generating water molecules as a primary source of moisture. With an increase in DFA/CE, water production shows a decreasing trend, suggesting that desulfurization ash may inhibit the bonding of hydroxyl groups and -H. Cellulose's pyrolysis leads to a char-forming reaction, where carbon-rich substances aggregate into char residues, releasing volatile gases—Char and Syngas are the main sources in CE pyrolysis products.

Table 4-9 indicates that LG pyrolysis results in the highest yield of char residues, as lignin is a high molecular weight compound formed by covalent bonding of phenylpropane monomers. The breaking and recombination of -C chains during pyrolysis lead to significant char residue production in LG. The tar yield decreases with an increase in DFA/LG, possibly due to desulfurization ash promoting the cleavage of carbon-hydrogen bonds, increasing the association of hydroxyl groups and hydrogen bonds, leading to an

increase in water yield.

4.4.1.2: Reaction mechanism of desulfurization ash on the catalytic reaction products of thermochemical gasification for model compounds

To further investigate the directed catalytic effect of desulfurization ash on different components in the thermochemical gasification of cotton stalks, CE and LG were selected as model compounds representing cellulose and lignin. The impact of blending ratios (DFA/CS, DFA/CE, DFA/LG) on the yields of various components in the gasification products is shown in the graph.

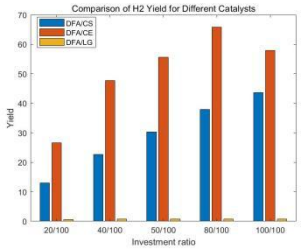

Table 4-10

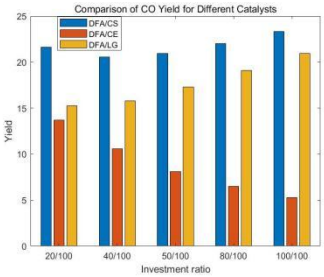

Table 4-11

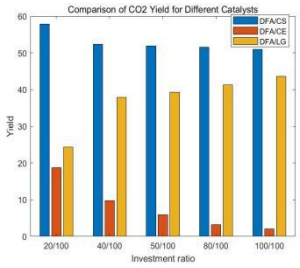

Table 4-12

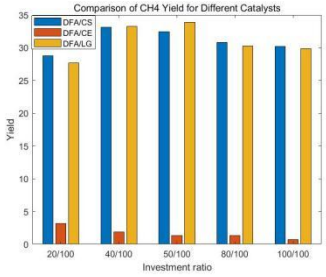

Table 4-13

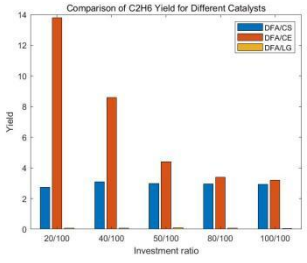

Table 4-14

Under the catalytic effect of desulfurization ash, the thermochemical gasification products of CE and LG exhibit significant differences in component yields. From Table 4-10, it is evident that the ranking of H2 production is DFA/CE > DFA/CS > DFA/LG, with H2 yields below 1.0 ml/g under different DFA/LG blending ratios. This demonstrates that H2 produced during cotton stalk pyrolysis mainly comes from the decomposition of CE. Desulfurization ash significantly promotes the chemical reactions producing hydrogen radicals, leading to the production of H2 during CE pyrolysis.

According to literature studies, the cleavage of ether bonds and carboxyl functional groups in the thermochemical biomass pyrolysis process of lignocellulosic materials is a major source of CO and CO2 in the gasification products.Table 4-11 andTable 4-12 show that both LG and CE are significant sources of CO and CO2 during cotton stalk pyrolysis. As the desulfurization ash blending ratio increases, its catalytic effect inhibits the reaction of CE breaking down to produce CO and CO2, leading to a continuous decrease in the production of these gases. Simultaneously, it promotes the reactions in LG, resulting in an increase in CO and CO2 production.

CH4 in DFA/CS gasification products mainly originates from the fracture of the methoxy side chains abundant in LG in cotton stalks. CE's pyrolysis produces minimal amounts of CH4, as shown in Table 4-14. Desulfurization ash exhibits a noticeable inhibitory effect on this process.

Table 4-14 reveals that LG's pyrolysis has difficulty producing C2H6, with C2H6 yields not exceeding 0.1 ml/g under various blending ratios. This is because, under low-temperature pyrolysis conditions, the aryl ring structure in LG is resistant to breaking. The main source of C2H6 in cotton stalk pyrolysis gas comes from the decomposition of CE,

where CE's structural units are further broken down into smaller free radicals to hinder the process of generating C2H6. With an increase in DFA/CE, C2H6 production decreases, indicating that desulfurization ash promotes the pyrolysis of CE, generating more free radicals of smaller molecular weight, inhibiting the process of CE structural unit cleavage and the formation of C2H6. However, with an increase in DFA/CS, C2H6 production does not change significantly, as there is mutual interaction between CE and LG molecules during pyrolysis, suppressing the radical reactions leading to C2H6. Therefore, under the combined influence of these factors, the gas yield in DFA/CS gasification is lower than that in DFA/CE gasification.

4.4.2 Establishment of Reaction Kinetics Models

We identified two approaches to formulate the kinetics equation for pyrolysis reactions through literature review. The literature provides substantial data supporting experimental conclusions, forming the basis for the kinetic equation used in the pyrolysis of sulfur removal ash catalyzed by CE and LG. However, for a more precise validation of the model, additional experimental data on the pyrolysis of sulfur removal ash catalyzed by CE and LG, such as temperature data, are required.

4.4.2.1 Biomass Weight Loss Rate Equation[3]

Drawing from the reference "Experimental Study on Process Parameters of Direct Pyrolysis Carbonization of Cotton Stalks," the literature employed a non-isothermal thermogravimetric analysis of cotton stalks, dynamically analyzing the weight loss relationship of the pyrolysis products. This led to the formulation of the biomass and its pyrolysis process equation:

$$A(s) \rightarrow B(s)+C(g) \tag{9}$$

Here, (A(s)) represents the biomass feedstock, (B(s)) is the solid product after pyrolysis, and (C(g)) is the gas product, including both gaseous and condensable liquid products.

α represents the percentage of sample weight loss at time t:

$$\alpha = \frac{m_0 - m_1}{m_0 - m_\infty} \tag{10}$$

The non-isothermal heterogeneous reaction kinetic equation for biomass weight loss is given as follows:

$$\frac{d\alpha}{dt} = k(T)f(\alpha) \tag{11}$$

Expressed in integral form:

$$g(\alpha) = kt \tag{12}$$

The reaction model parameters (f(α)) and (g(α)) are obtained by fitting the data to the Arrhenius equation, where (R) is the ideal gas constant (8.314 kJ/mol), (T) is the thermodynamic temperature.

$$\mathrm{In}\frac{g(\alpha)}{T^2} = \mathrm{In}[\frac{AR}{\beta E_a}] - \frac{E_a}{RT} \tag{13}$$

$$\beta = \frac{dT}{dt} \tag{14}$$

$\mathrm{In}\frac{g(\alpha)}{T^2}, \frac{1}{T}$ is a straight line, and E and A are calculated from the slope and intercept of the line.

So that's the weight loss rate equation we got for biomass.

4.4.2.2 Isothermal Heterogeneous Reaction Kinetics Pyrolysis Equation[4]

By referencing "Mechanism Study on Low-Temperature Melting Nitrate Pyrolysis of Woody Cellulosic Biomass" by Yang Yuhang, we employed a melting salt reaction kettle

and process mass spectrometry coupling method to solve the isothermal heterogeneous reaction kinetics pyrolysis equation. This approach provides parameters and reaction mechanisms that closely approximate intrinsic values. The reaction mechanism function (G(x)) is as follows:

$$G(x) = \int_0^x \frac{dx}{f(x)} = k(T)t \tag{15}$$

Where (k(T)) is the reaction rate constant, and (f(x)) is the differential form of the reaction mechanism function.

Subsequent steps involve fitting experimental data for the pyrolysis of sulfur removal ash catalyzed by CE and LG to evaluate the performance of each experimental model.

4.5 Modeling of question five

4.5.1Nonlinear regression model

According to the simple fitting of the data accumulated in the first three questions and the dynamics model and reaction mechanism model of the relevant data consulted in question 4, we used MATLAB to carry out a more accurate nonlinear regression fitting model, and the image results obtained are as follows：

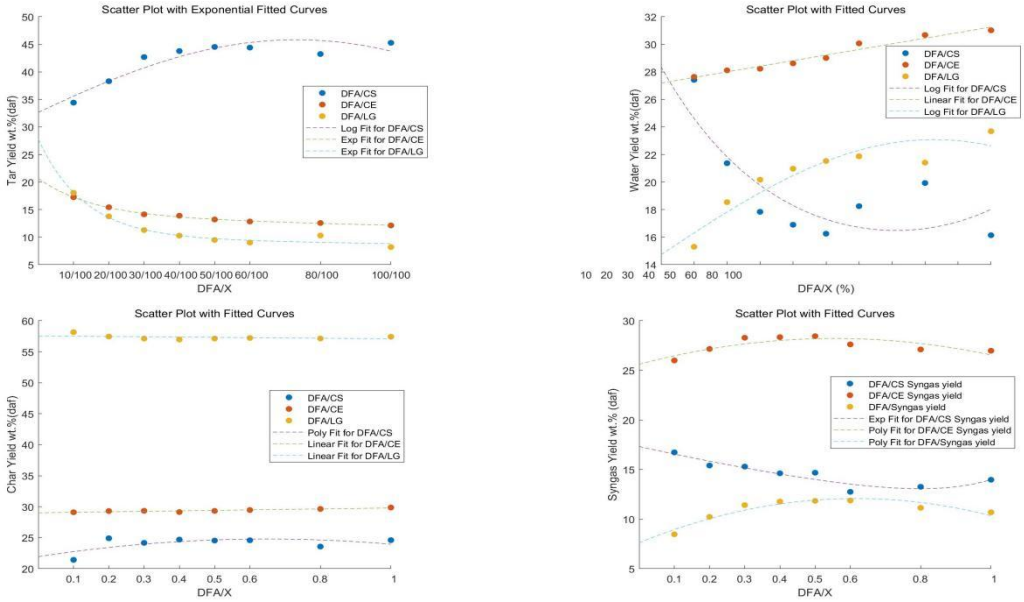

Nonlinear regression prediction for the pyrolysis products of Appendix I

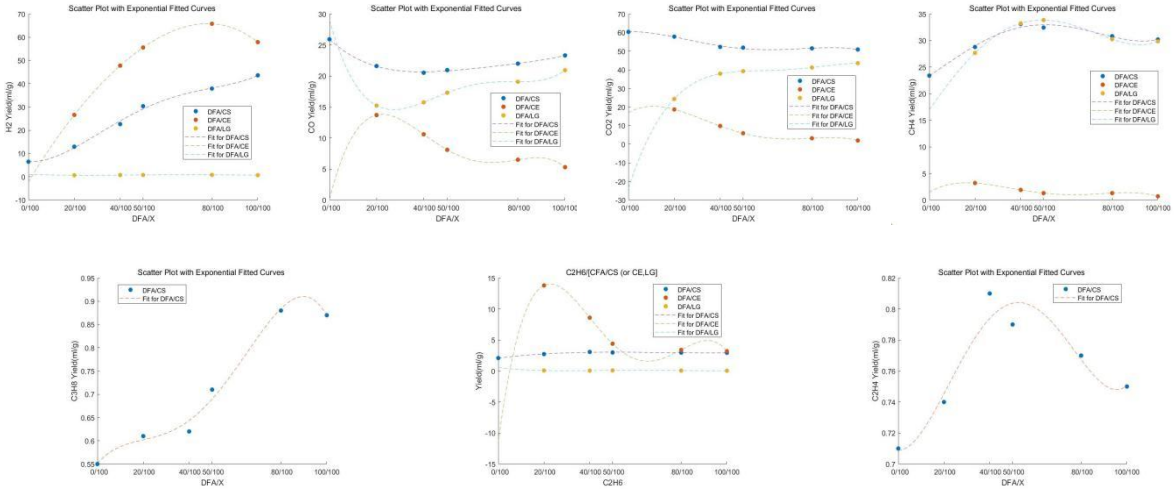

Nonlinear regression prediction for different pyrolysis gases in Appendix II

The nonlinear regression models used are collected in appendix.

4.5.2Grey Prediction Model

The Grey Prediction Model (GPM) is a mathematical model employed in the fields of system identification, prediction, and decision analysis, especially when dealing with limited data. This model is designed to make predictions based on a small amount of available data.

Based on SPSS, we can draw the model fitting prediction graph[5]:

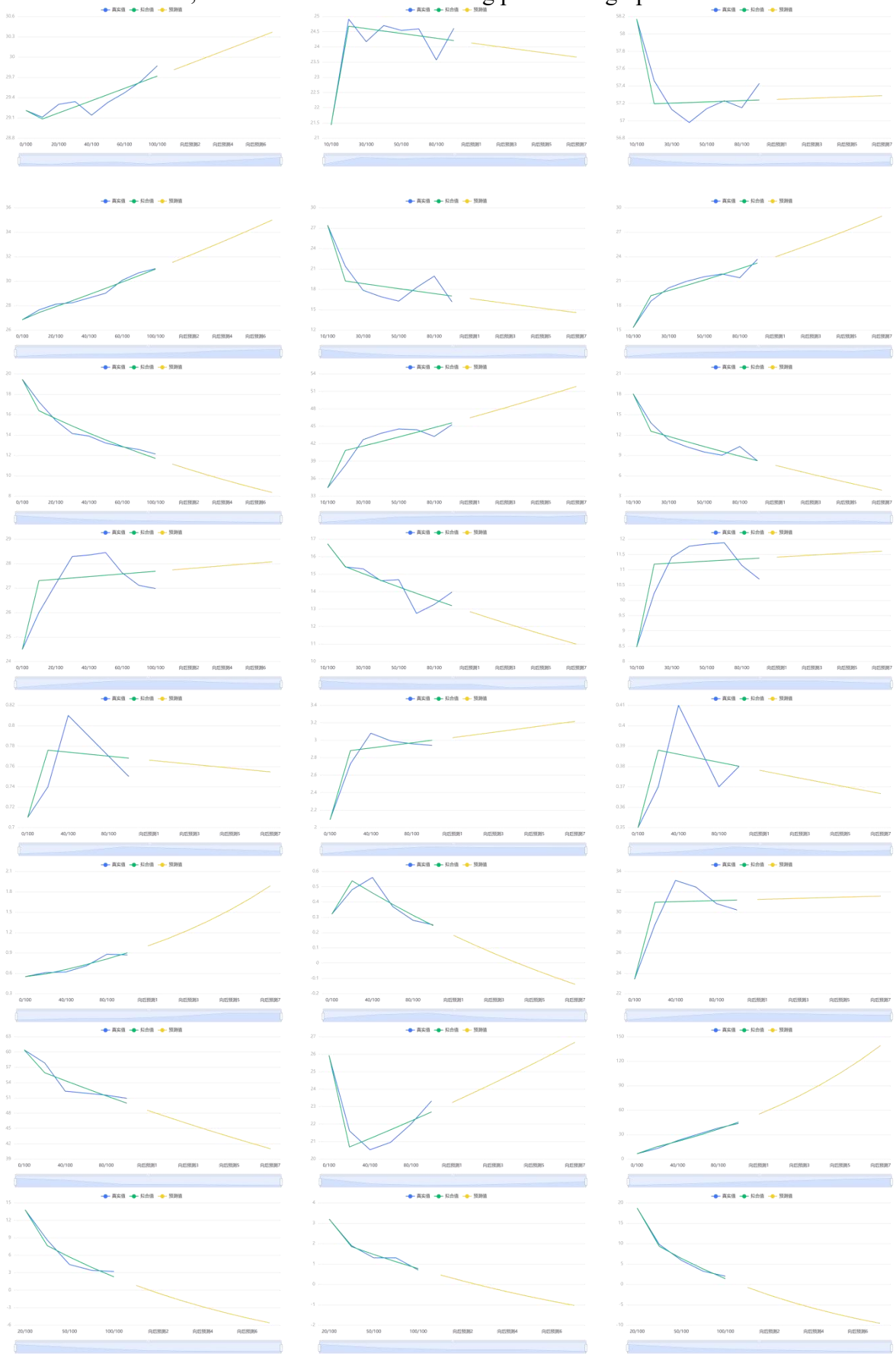

According to the images and related predictions, it can be seen that the data of the gray prediction model fits the original data to a high degree, so the model we obtained is relatively accurate and can be used as a prediction model to predict the pyrolysis yields of different combinations and different gases under different pyrolysis reactions.

5.Test the Models

In consideration of the aforementioned Grey Prediction Model, residual analysis was conducted to assess the model's fitting adequacy.

Residual analysis is a common tool in mathematical modelling for assessing model fit and checking model assumptions. Residuals are the differences between the observed values and the predicted values of the model, and residual analysis assesses the accuracy and reliability of the model by analysing these differences statistically and graphically.

From SPSS and Excel, we can get the graph:

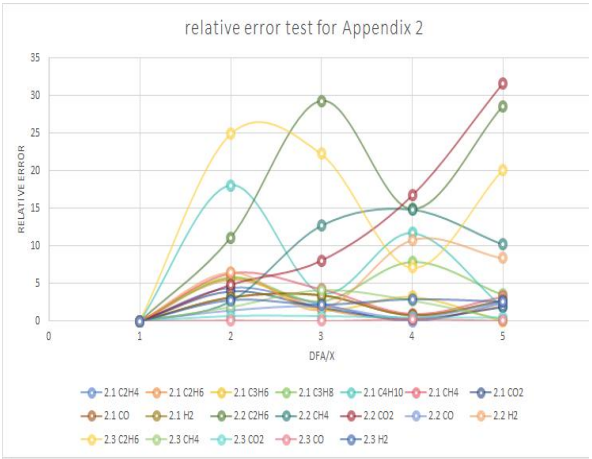

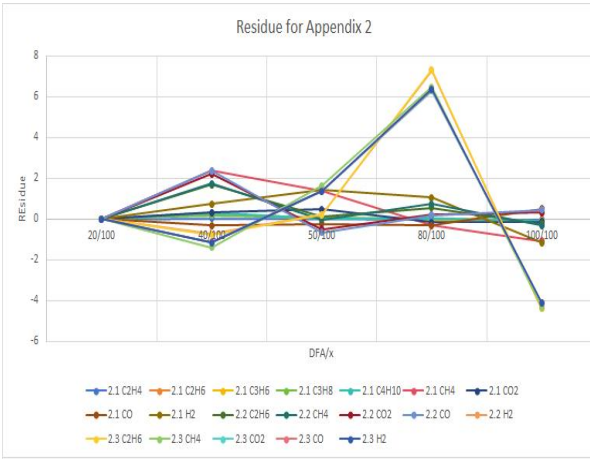

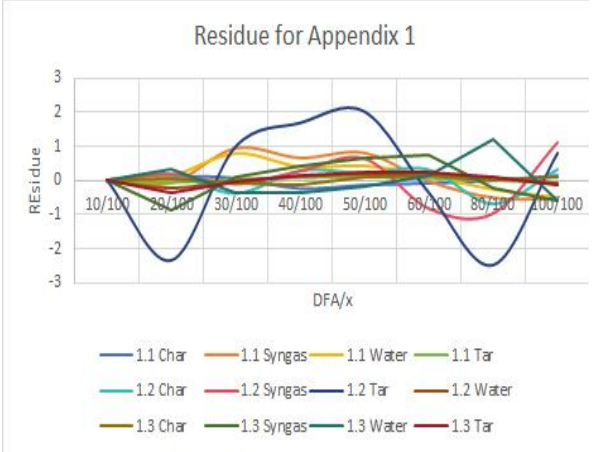

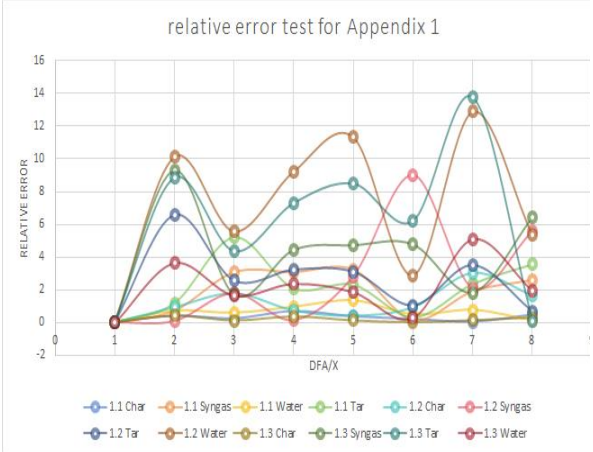

From the four figures above, it is evident that the table above illustrates the fitting results of the Grey Prediction Model. A smaller relative error value indicates a better fit, typically considered satisfactory when below 20%. The average relative error of the model is also around 5%-9%, indicating a good fit. This further validates the high degree of fitting achieved by our model.

In addition, some residual values still exist. We conducted residual plot analysis for all data using MATLAB, revealing curves with relatively low fitting degrees as follows：

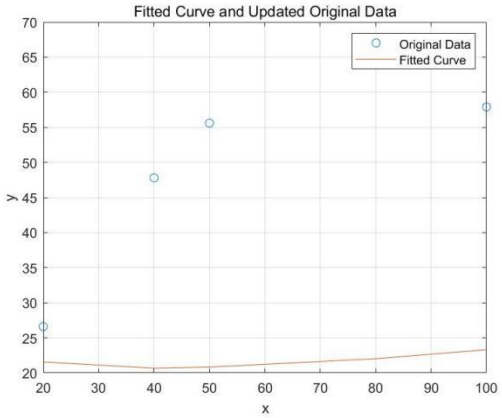

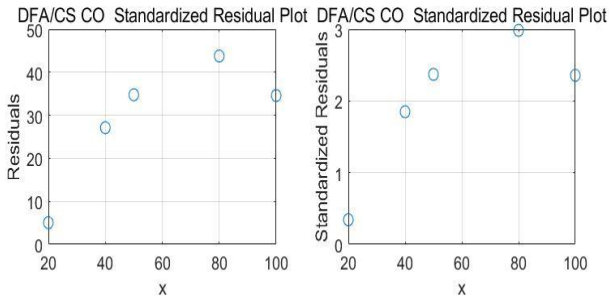

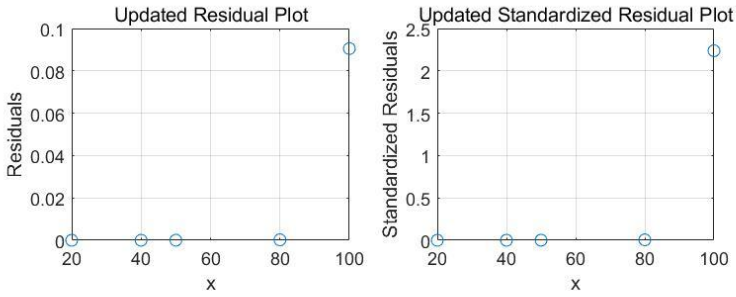

"This also indicates that the yield of certain products is not only influenced by the univariate factor of feed ratio but may also be affected by other factors. Relying solely on this model may pose some limitations. Upon reviewing relevant literature, it is evident that factors such as reaction temperature, pressure, activation energy, and intermediate products may play a role. We have addressed this aspect in question four as well."

6.Strengths and Weakness

6.1 Model Advantages

In addressing questions one and two, the statistical analysis offers the advantage of convenient graphical representation, with clear trends. Correlation analysis is easily computable and interpretable, measuring the strength and direction of linear relationships.

For the t-test in question three, the model excels in reducing individual variation, enhancing statistical efficiency.

In question four, a thorough examination of relevant literature provides robust supplementary evidence and arguments for the essence of the reactions.

In question five, employing various forms of univariate regression enhances the precision of the model.

6.2 Model Limitations

Concerning the t-test in question three, the model's drawbacks include the need for extensive experimental design and data collection, making it time-consuming and labor-intensive. The choice of pairing conditions demands high precision, introducing potential subjectivity and errors. Additionally, single-factor analysis of variance imposes requirements on data normality and homogeneity of variance; non-compliance may lead to inaccurate results. In question five, the model's accuracy diminishes with the introduction of additional variables due to a lack of corresponding data.

6.3 Model Improvement

To enhance the model in question three, stricter pairing conditions could be considered, or alternative statistical methods could be integrated to improve the reliability and efficiency of matched-sample t-tests. Furthermore, non-parametric methods can be applied in single-factor analysis of variance to address issues of data normality and homogeneity of variance. For question five, seeking additional experimental data related to other variables associated with the thermal decomposition reaction and establishing a multivariate regression model can elevate the model's accuracy.

7.Conclusion

In this study, we investigate distinctive features and their root causes. Initially, the existing data is examined through trend analysis, correlation analysis, and linear programming. Subsequently, differential analysis is performed using t-tests and analysis of variance. Lastly, a nonlinear regression model is developed and verified through algorithms, showcasing the logical and precise nature of the mathematical model.

Although the model used is relatively simple, we have tested it and reviewed a lot of literature to supplement and refine the paper.

References

[1] [1] Scientific Platform Serving for Statistics Professional 2021. SPSSPRO. (Version 1.0.11)[Online Application Software]. Retrieved from https://www.SPSSpro.com.

[2] Du Qi, TANG Chuyang, An Xinyuan et al. Study on catalytic extraction of biomass pyrolysis gas from desulfurization ash based on model compounds [J]. Renewable Energy, 2019,41(06))

[3] Axel F, Felix Zr Heat of reaction measurements for hydrothermal carbonization ofbiomass. Bioresource Technology,2011,102 (16) :7595-7598

[4] Burkhard K. Werner H, Friedhelm B. Catalytic hydroliquifaction of biomass.Fuel1999,69 (4) :448-455

[5] Scientific Platform Serving for Statistics Professional 2021. SPSSPRO. (Version 1.0.11)[Online Application Software]. Retrieved from https://www.spsspro.com.

[6] LU Dangzhen, Yao Hong, Wang Quanbin et al. Experimental study on Effects of cellulose and lignin content on pyrolysis and gasification characteristics of biomass [J]. Journal of Engineering Thermophysics,2008,(10):

[7] LIAO Y F. Experimental study on pyrolysis mechanism of cellulose [D]. Zhejiang University,2003. (in Chinese)

[8] Jin, LI Baoxia. Co-pyrolysis of cellulose and lignin [J]. Journal of Chemical Industry,2013,32(02):

[9] Study on Structure and pyrolysis of cotton stalk [J].Agricultural Science Technology,2011,12(02):

[10] Chen Mingqiang, QI Xueyi, Wang Jun et al. Study on catalytic pyrolysis characteristics and kinetic modeling of cotton stalk [J]. Journal of Fuel Chemistry and Technology,2011,39(08):

[11] Song Chuncai, Hu Haoquan. Study on catalytic pyrolysis and kinetics of straw and its main components [J]. Coal Conversion,2003,(03):

Appendix

Statistical analysis of data preprocessing：

Variable Name	Sample Size	Max	Min	Mean	Standard Deviation	Median	Variance	Kurtosis	Skewness	Coefficient of Variation （CV）
Tar yield	9	19.46	12.13	14.547	2.431	13.89	5.909	0.784	1.225	0.167
Char yield	9	29.87	29.11	29.379	0.246	29.33	0.061	0.678	1.058	0.008
Water yield	9	31.02	26.84	28.913	1.415	28.62	2.003	-1.035	0.259	0.049
Syngas yield	9	28.45	24.49	27.161	1.279	27.16	1.635	1.357	-1.174	0.047

TAB1

Variable name	Sample size	Max	Min	Mean	Standard Deviation	Median	Variance	Kurtosis	Skewness	Coefficient of Variation （CV）
Tar yield	8	18.06	8.19	11.3	3.207	10.29	10.284	2.423	1.583	0.284
Water yield	8	23.69	15.3	20.435	2.539	21.19	6.446	1.926	-1.192	0.124
Char yield	8	58.17	56.98	57.336	0.373	57.19	0.139	4.045	1.885	0.007
Syngas yield	8	11.88	8.47	10.929	1.153	11.275	1.33	2.631	-1.6	0.106

TAB2

Variable name	Sample size	Max	Min	Mean	Standard Deviation	Median	Variance	Kurtosis	Skewness	Coefficient of Variation （CV）
Tar yield	8	18.06	8.19	11.3	3.207	10.29	10.284	2.423	1.583	0.284
Water yield	8	23.69	15.3	20.435	2.539	21.19	6.446	1.926	-1.192	0.124
Char yield	8	58.17	56.98	57.336	0.373	57.19	0.139	4.045	1.885	0.007
Syngas yield	8	11.88	8.47	10.929	1.153	11.275	1.33	2.631	-1.6	0.106

TAB3

Significance test form

Variable Name	Sample Size	Median	Mean	Standard Deviation	Skewness	Kurtosis	Shapiro-Wilk Test	Kolmogorov-Smirnov Test
H2	6	26.5	25.662	14.379	-0.142	-1.522	0.964(0.852)	0.145(0.997)
CO	6	21.805	22.39	1.984	1.352	1.624	0.884(0.287)	0.245(0.791)
CO2	6	52.115	54.152	3.96	1.086	-0.831	0.798(0.056*)	0.346(0.381)
CH4	6	30.52	29.8	3.495	-1.448	2.381	0.877(0.257)	0.22(0.880)
C2H6	6	2.95	2.798	0.366	-1.958	3.945	0.757(0.023**)	0.317(0.483)
C3H6	6	0.375	0.378	0.02	0.333	0.516	0.975(0.926)	0.175(0.976)
C3H8	6	0.665	0.707	0.14	0.454	-1.96	0.875(0.249)	0.232(0.839)
C2H4	6	0.76	0.762	0.036	-0.086	-0.641	0.99(0.988)	0.127(1.000)
C4H10	6	0.345	0.377	0.121	0.706	-0.99	0.926(0.550)	0.189(0.955)

Note: ***, ** and * represent significance levels of 1%, 5% and 10% respectively

Variable Name	Sample Size	Median	Mean	Standard Deviation	Skewness	Kurtosis	Shapiro-Wilk Test	Kolmogorov-Smirnov Test
H2	5	55.6	50.74	14.942	-1.273	1.887	0.909(0.461)	0.228(0.907)
CO	5	8.1	8.84	3.364	0.686	-0.634	0.954(0.767)	0.187(0.981)
CO2	5	5.9	7.92	6.73	1.283	1.3	0.889(0.354)	0.218(0.929)
CH4	5	1.3	1.68	0.95	1.202	1.686	0.904(0.435)	0.255(0.827)
C2H6	5	4.4	6.68	4.54	1.241	0.453	0.836(0.153)	0.292(0.694)

Note: ***, ** and * represent significance levels of 1%,
5% and 10% respectively

Variable Name	Sample Size	Median	Mean	Standard Deviation	Skewness	Kurtosis	Shapiro-Wilk Test	Kolmogorov-Smirnov Test
H2	5	0.78	0.754	0.058	-0.85	-0.888	0.907(0.453)	0.274(0.764)
CO	5	17.305	17.661	2.365	0.524	-1.329	0.943(0.685)	0.189(0.978)
CO2	5	39.26	37.262	7.526	-1.791	3.548	0.813(0.102)	0.334(0.529)
CH4	5	30.26	30.982	2.557	-0.064	-1.65	0.929(0.591)	0.212(0.940)
C2H6	5	0.07	0.07	0.016	0	-1.2	0.987(0.967)	0.136(1.000)

Note: ***, ** and * represent significance levels of 1%, 5% and 10% respectively

Linear and quadratic fit equations for problem 1：

	Yield Type	Number of Fits	Fitted Equation	R^2-Value
DFA/CS	H2	1	$y = 0.3831x + 7.1465$	0.9770
		2	$y=-0.0013x^2 + 0.5111x + 5.3516$	0.9865
	CO	1	$y = -0.0146x + 23.0936$	0.0741
		2	$y = 0.0016x^2 -0.1803x+25.4182$	0.9107
	CO2	1	$y = -0.0938x + 58.6834$	0.7718
		2	$y = 0.0015x^2 + -0.2462x + 60.8210$	0.9495
	CH4	1	$y = 0.0535x + 27.2153$	0.3224
		2	$y = -0.0025x^2 +0.3026x+23.7216$	0.9317
	C2H6	1	$y = 0.0068x + 2.4712$	0.4715
		2	$y = -0.0002x^2 + 0.0294x +2.1543$	0.9294
	C3H8	1	$y = 0.0036x + 0.5314$	0.9228
		2	$y = 0.0001x^2 + 0.0030x + 0.5403$	0.9253
	C3H6	1	$y = 0.0002x + 0.3700$	0.0976
		2	$y = -0.0000x^2 + 0.0015x +0.3515$	0.5986
	C2H4	1	$y = 0.0004x + 0.7447$	0.1309
		2	$-0.0000x^2 + 0.0031x + 0.7057$	0.8454
	C4H10	1	$y = -0.0016x + 0.4562$	0.2559
		2	$y = -0.0001x^2 + 0.0052x + 0.3602$	0.6412
DFA/CE	H2	1	$y = 0.3832x + 28.5152$	0.6708
		2	$y = -0.0119x^2 + 1.8261x -5.6417$	0.9971
	CO	1	$y = -0.1006x + 14.6770$	0.9127
		2	$y = 0.0012x^2 -0.2491x+18.1917$	0.9809
	CO2	1	$y = -0.1911x + 19.0054$	0.8228
		2	$y = 0.0038x^2 +-0.6496x+29.8583$	0.9852
	CH4	1	$y = -0.0265x + 3.2181$	0.7953
		2	$y = 0.0005x^2 + -0.0824x +4.5417$	0.9166
	C2H6	1	$y = -0.1238x + 13.8618$	0.7587
		2	$y = 0.0029x^2 -0.4726x+22.1167$	0.9652
DFA/LG	H2	1	$y = 0.0016x + 0.6639$	0.7396
		2	$y = -0.00001x^2 +0.0060x+0.5575$	0.9518
	CO	1	$y = 0.0731x + 13.4239$	0.9734
		2	$y = 0.0003x^2 + 0.0383x +14.2467$	0.9810
	CO2	1	$y = 0.1997x + 25.6788$	0.7183
		2	$y = -0.0048x^2 +0.7849x+11.8258$	0.9299
	CH4	1	$y = -0.0001x + 30.9902$	3.1525e-06
		2	$y = -0.0030x^2 +0.3619x+22.4192$	0.7017
	C2H6	1	$y = -0.0003x + 0.0871$	0.3529
		2	$y = -0.0000x^2 + 0.0006x+0.0650$	0.4745

	Yield Type	Number of Fits	Fitted Equation	R^2-Value

DFA/CS	Tar	1	y= -0.0654x+17.3825	0.7791
		2	y= $0.0011x^2$-0.1710x+18.9240	0.9694
	Water	1	y= 0.0425x + 27.0732	0.9678
		2	y= $-0.0001x^2$+0.0521x+26.9329	0.9724
	Char:	1	y= 0.0067x + 29.0865	0.8063
		2	y= $0.0001x^2$+-0.0007x+29.1948	0.8977
	Syngas:	1	y= 0.0162x + 26.4579	0.1732
		2	y=$-0.0010x^2$+0.1196x+24.9484	0.8326
DFA/CE	Tar	1	y = 0.0938x + 37.5105	0.5754
		2	y = $-0.0025x^2$ + 0.3633x + 32.2226	0.8662
	Water	1	y = -0.0746x + 22.8971	0.3647
		2	y = $0.0024x^2$ + -0.3369x + 28.0436	0.6409
	Char:	1	y = 0.0138x + 23.3943	0.1732
		2	y=$-0.0007x^2$ + 0.0879x + 21.9392	0.3743
	Syngas:	1	y = -0.0330x + 16.1981	0.6245
		2	y= $0.0007x^2$ -0.1144x + 17.7945	0.8570
DFA/LG	Tar	1	y = -0.0836x + 15.3758	0.6300
		2	y = $0.0019x^2$ + -0.2940x + 19.5045	0.8742
	Water	1	y = 0.0722x + 16.9141	0.7500
		2	y = $-0.0011x^2$ + 0.1926x + 14.5517	0.8875
	Char:	1	y = -0.0048x + 57.5717	0.1555
		2	y = $0.0004x^2$ + -0.0435x + 58.3300	0.7648
	Syngas:	1	y = 0.0162x + 10.1383	0.1832
		2	y = $-0.0012x^2$ + 0.1449x + 7.6138	0.1832

The equation of nonlinear regression fitting is adopted for problem 5：

Table2H2	Fit for DFA/CS: 0.0000016460*x^4 + -0.0003654729*x^3 + 0.0243751612*x^2 + -0.0587543049*x + 6.5632039595
	Fit for DFA/CE: -0.0000004236*x^4 + 0.0000527083*x^3 + -0.0116152778*x^2 + 1.6601666667*x + -2.3111111111
	Fit for DFA/LG: 0.0000000493*x^4 + -0.0000133958*x^3 + 0.0011809722*x^2 + -0.0367666667*x + 1.0322222222
Table2CO	Fit for DFA/CS: 0.0000002805*x^4 + -0.0000772974*x^3 + 0.0082031917*x^2 + -0.3541308539*x + 25.9383641931
	Fit for DFA/CE: -0.0000027361*x^4 + 0.0006545833*x^3 + -0.0524611111*x^2 + 1.4881666667*x + 0.1222222222
	Fit for DFA/LG: 0.0000020253*x^4 + -0.0004957187*x^3 + 0.0419853472*x^2 + -1.3476500000*x + 29.0305555556
Table2CO2	Fit for DFA/CS: -0.0000011736*x^4 + 0.0002377113*x^3 + -0.0134220393*x^2 + 0.0431995051*x + 60.4352236149
	Fit for DFA/CE: -0.0000026181*x^4 + 0.0005918750*x^3 + -0.0415430556*x^2 + 0.7045000000*x + 16.9111111111
	Fit for DFA/LG: -0.0000028368*x^4 + 0.0008117708*x^3 + -0.0838493056*x^2 + 3.7764166667*x + -23.6788888889
Table2CH4	Fit for DFA/CS: 0.0000006204*x^4 + -0.0000992306*x^3 + 0.0015576230*x^2 + 0.2847318165*x + 23.3729155391
	Fit for DFA/CE: -0.0000007153*x^4 + 0.0001581250*x^3 + -0.0112902778*x^2 + 0.2555000000*x + 1.4555555556
	Fit for DFA/LG: 0.0000007903*x^4 + -0.0001044583*x^3 + -0.0023355556*x^2 + 0.6167833333*x + 16.9777777778

Table2C2H6	Fit for DFA/CS: 0.0000000023*x^4 + 0.0000028242*x^3 + -0.0006764187*x^2 + 0.0456370709*x + 2.0861650762
	Fit for DFA/LG: -0.0000028368*x^4 + 0.0008117708*x^3 + -0.0838493056*x^2 + 3.7764166667*x + -23.6788888889
	LOG Fit for DFA/CE: y = 0.0003 * x^2 + -0.0536 * x + 3.6242
Table2C3H8	-0.0000000319*x^4 + 0.0000054207*x^3 + -0.0002474352*x^2 + 0.0055695995*x + 0.5514207378
Table2C2H4	0.0000000144*x^4 + -0.0000028562*x^3 + 0.0001462085*x^2 + -0.0000806651*x + 0.7090343256

Tar	CS logarithm Exp Fit for DFA/CS: 45.2186*exp(-0.0045*x)
	CE exponential Exp Fit for DFA/CE: 6.7857*exp(-0.0647*x)
	LG exponential Exp Fit for DFA/LG: 17.8744*exp(-0.0763*x)
Water	CS exponential Exp Fit for DFA/CS: 30.4472exp(-0.1032x)
	CE Linear Fit for DFA/CE: 0.0407 + 27.1877x
	LG logarithm Log Fit for DFA/LG: -0.0001 + 0.0109x
Char	CS Poly Fit for DFA/CS: -0.0007 + 0.0879x + 21.9392x^2
	CE Linear Fit for DFA/CE: 0.0077 + 29.0258x
	LG Linear Fit for DFA/LG: -0.0048 + 57.5717x
Syngas	CS exponential Exp Fit for DFA/CS Syngas yield: 17.3051 * exp(-0.0045 * x)
	CE Poly Fit for DFA/CE Syngas yield: -0.0008 + 0.0935x + 25.6182x^2
	LG Poly Fit for DFA/Syngas yield: -0.0012 + 0.1449x + 7.6138x^2